Surface & Coatings Technology 434 (2022) 128205

Contents lists available at ScienceDirect

Surface & Coatings Technology

journal homepage: www.elsevier.com/locate/surfcoat

Microstructure and tribological properties of Al_2O_3 reinforced FeCoNiCrMn high entropy alloy composite coatings by cold spray

Yongming Zou [a,b], Zhaoguo Qiu [b], Chunjie Huang [c], Dechang Zeng [b], Rocco Lupoi [a], Nannan Zhang [d,*], Shuo Yin [a,*]

[a] Department of Mechanical, Manufacturing and Biomedical Engineering, Trinity College Dublin, The University of Dublin, Parsons Building, Dublin 2, Ireland
[b] School of Materials Science and Engineering, South China University of Technology, Guangzhou 510640, China
[c] Institute of Materials Technology, Helmut-Schmidt-University/University of the Federal Armed Forces Hamburg, 22043 Hamburg, Germany
[d] Department of Material Science and Engineering, Shenyang University of Technology, Shenyang 110870, Liaoning, China

ARTICLE INFO

Keywords:
Cold spray (CS)
High entropy alloys (HEAs)
Composite coatings
Microstructure
Mechanical properties
Tribological properties

ABSTRACT

High entropy alloys (HEAs) are novel materials that have been extensively studied in recent years. In this work, Al_2O_3 particles reinforced FeCoNiCrMn HEA composite coatings were fabricated by cold spray. The microstructure, mechanical and tribological properties of the composites coating were studied and compared with those of the pure FeCoNiCrMn coating. The results indicate that cold spray is a promising process to fabricate HEA composite coatings. The composite coatings made in this work had higher hardness than pure FeCoNiCrMn coating due to the reinforcing effect of well distributed Al_2O_3 particles. The composite coatings also had improved wear-resistance properties with nearly 50% reduction in wear rate as compared to the pure FeCoNiCrMn coating. The improvement was due to the formation of tribo-layer which can effectively withstand material loss. The results also reveal that the main wear mechanisms for the composite coatings were dominated by adhesive wear in comparison to abrasive wear for the pure FeCoNiCrMn coating. This study proves the feasibility of cold spray for the fabrication of high-performance HEA composite coatings.

1. Introduction

High entropy alloys (HEAs) consist of multicomponent and equiatomic metal elements such as Fe, Co, Ni, Cr, Mn, Mo, Al, Ti. The configurational entropy of mixing elements in HEAs leads to the formation of single or multiple solid solutions with body centered cubic (BCC) or face centered cubic (FCC) structure, which breaks the "one main element" design concept of traditional alloys. Therefore, HEAs normally exhibit excellent strength and ductility, high damage-tolerance, superior oxidation and corrosion resistance, and outstanding wear resistance [1–3].

Among various HEAs, FeCoNiCrMn with FCC structure shows great potential in cryogenic and high-temperature applications, and corrosion-/wear-resistance fields [4–8]. Recently, several thermal spraying techniques including laser cladding [9], high velocity air/oxygen fuel spray [10–12], magnetron sputter [13], plasma spray [14], and plasma cladding [15] have been applied to fabricate HEA coatings for substrate protection. For example, Ye et al. [16] reported a much higher corrosion resistance of laser cladded FeCoNiCrMn HEA coatings as compared to 304 stainless steel through potentiodynamic polarization and electrochemical impedance spectroscopy tests in 0.5 M sulfuric acid and 3.5 wt % NaCl solution. Xiao et al. [14] studied the tribological properties of plasma sprayed FeCoNiCrMn coatings before and after annealing, and found that the FeCoNiCrMn coatings had rather high wear-resistance performance which can be further improved via annealing treatment on the coatings. Other thermally sprayed FeCoNiCrMn coatings also exhibited good wear-resistance performance as reported in literature [17–20]. In recent years, HEA-based composite coatings were also extensively studied. Zhang et al. [19] investigated the microstructure and mechanical properties of plasma sprayed FeCoNiCrMn composite coatings reinforced by Al_2O_3 and TiO_2 particles. They found that the composite coatings had significantly improved wear resistance as compared to the pure HEA coatings due to the reinforcing particles that resulted in high resistance of the coating against deformation and crack propagation. Peng et al. [21] investigated the effect of WC content on the microstructure and mechanical properties of FeCoCrNi-WC composite coatings fabricated by plasma cladding. A hardness of 59.6 HRC and a wear rate of 3.27×10^{-7} $mm^3/N{\cdot}m$ were achieved when the

* Corresponding authors.
E-mail addresses: zhangnn@sut.edu.cn (N. Zhang), yins@tcd.ie (S. Yin).

https://doi.org/10.1016/j.surfcoat.2022.128205
Received 8 January 2022; Received in revised form 1 February 2022; Accepted 3 February 2022
Available online 7 February 2022

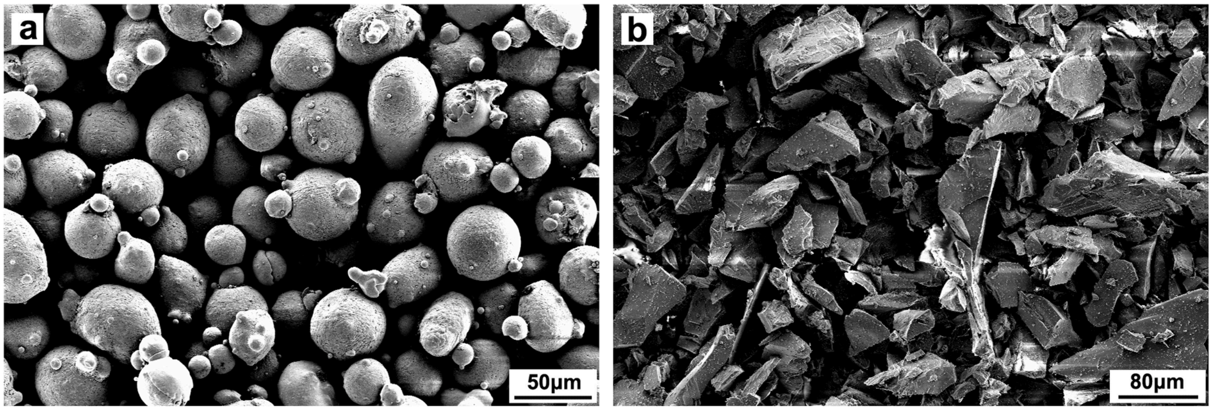

Fig. 1. SEM images of the powder materials: (a) FeCoNiCrMn powder, and (b) Al_2O_3 particle.

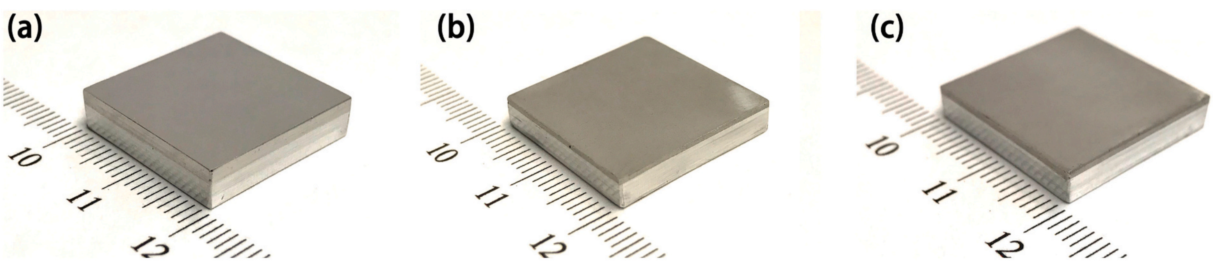

Fig. 2. Photos of the as-deposited coatings: (a) pure FeCoNiCrMn coating (b) Composite-1 coating (c) Composite-2 coating.

content of WC was 60 wt%. The excellent wear resistance arose from the friction reduction effect caused by WC particles and the formation of Fe_3W_3C carbide phase in the composite coatings. Despite widely used, thermal spray techniques usually result in the occurrence of phase transformation, oxidation and elements segregation in the coatings due to high processing temperature, which may cause deterioration of mechanical properties [13,22,23].

Cold spray is a solid-state deposition technique, in which microparticles are accelerated to 300– 1200 m/s by high-temperature compressed gases and then deposit on substrates to form coatings at a temperature well below the particle melting temperature [24–26]. The low deposition temperature prevents the formation of defects associated with high temperature. Zhang et al. [27] compared cold spray to atmospheric plasma spray, reporting that cold sprayed Inconel 718 coatings were denser and harder with less oxidizations. Therefore, cold spray is also a promising candidate for fabricating HEA coatings. However, currently, there are only few studies focusing on the microstructure, deposition mechanism and properties of cold sprayed HEA coatings [23,28], while no research was conducted to investigate ceramic-reinforced HEA composite coatings yet. Considering the advantages provided by cold spray and ceramic reinforcements, in this work, we applied cold spray to fabricate Al_2O_3-reinforced FeCoNiCrMn composite coatings and studied their microstructures and tribological performance.

2. Experimental details

2.1. Feedstock and cold spray process

Spherical FeCoNiCrMn HEA powder with the size ranging from 15 to 53 μm (Vilory Advanced Materials Technology Ltd., China) and angular Al_2O_3 powders with the size range of 53 to 75 μm (Kuhmichel, Germany) were chosen as the feedstock. The SEM morphologies of the feedstock are shown in Fig. 1. The spherical shape of the FeCoNiCrMn HEA powder is benefit to the particle deformation and interparticle bonding, while the angular shape of the Al_2O_3 particle make them easy to embed into substrate or formed coating layer. The two powders were mechanically mixed at the weight ratio of 8:1 and 4:1.

Pure FeCoNiCrMn and composite coatings with the thickness of over 1.5 mm were deposited on 6082 Al alloy substrates by using an in-house cold spray system (Trinity College Dublin, Ireland) [29]. For convenience, the two composite coatings were denoted as Composite-1 for 11 wt% Al_2O_3 reinforced coating and Composite-2 for 20 wt% Al_2O_3 reinforced coating, respectively. Compressed helium gas with the pressure of 3 MPa and temperature of 300 °C was used as the accelerating gas. In addition, the spraying distance and nozzle traversal speed were set as 30 mm and 100 mm/s, respectively. The as-deposited coatings were subsequently cut into cubic blocks with a dimension of $20 \times 20 \times 5$ mm^3 for tribological properties tests as shown in Fig. 2.

2.2. Material characterizations

The microstructure and worn surface of the as-deposited coatings were characterized by field emission scanning electron microscope (FE-SEM, FEO NOVA 430). As for the microstructure characterization, the specimens were prepared following standard metallographic procedures and etched in HCl (15 mL) + HNO_3 (5 mL) solution for 30 s. The volume fraction of Al_2O_3 in the as-deposited coatings was measured by Image J. Electron backscatter diffraction (EBSD, OXFORD NORDLYS X-MAX) was used to investigate the grain structure evolution of the composite coatings. The EBSD analysis system was operated at an accelerating 20 kV with an inclination angle of 70° and a step length of 0.15 um.

2.3. Microhardness and wear tests

The microhardness of the as-deposited coatings was measured by a hardness tester (ZHU0.2, Zwick/Roell Instruments, Germany) with a load of 300 g and a hold time of 10 s (HV0.3). For each specimen, the microhardness was calculated by averaging the results of 15 indentations, which were made at randomized positions on polished cross-

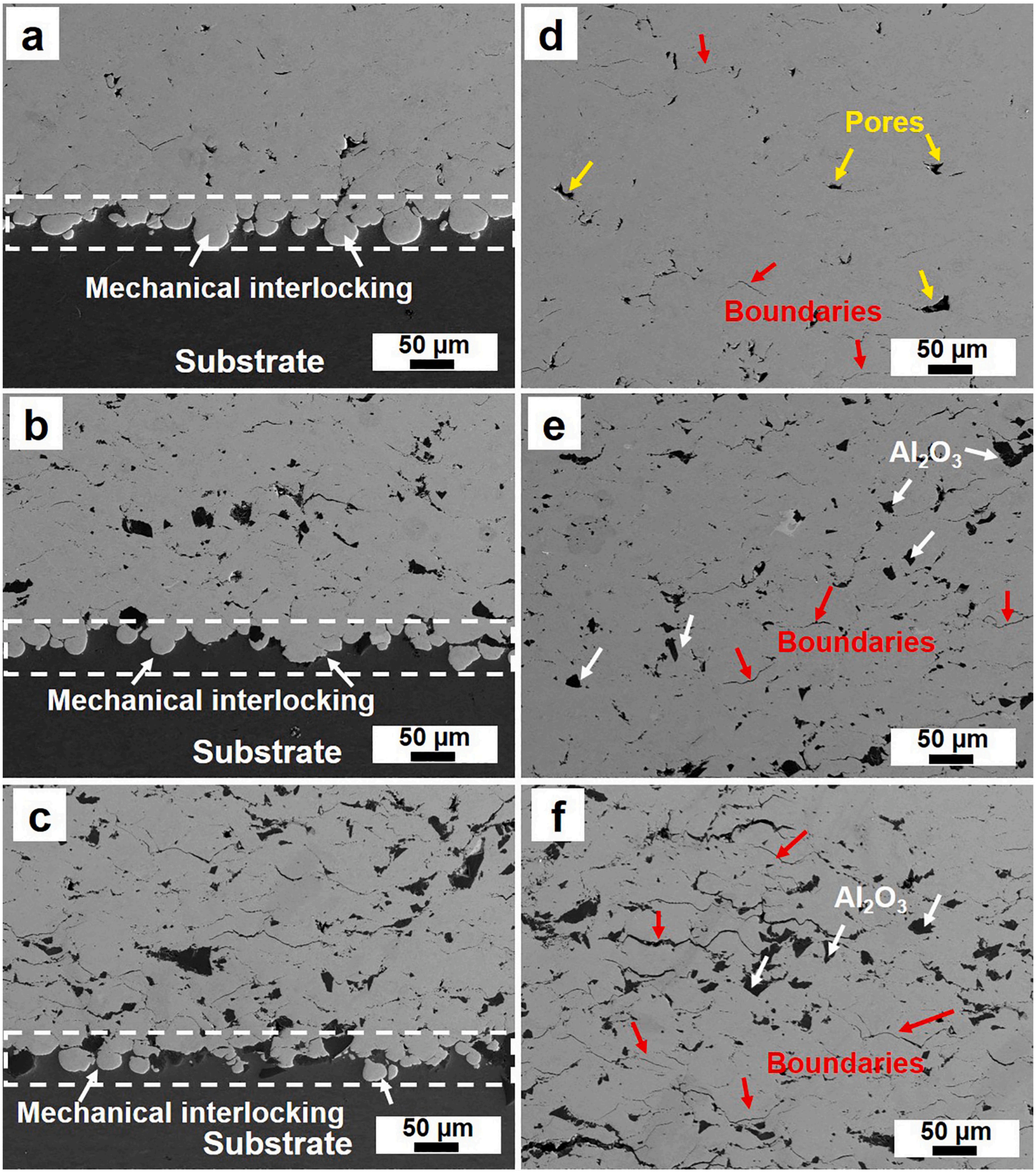

Fig. 3. Cross-section SEM images of the coating-substrate interfaces and the coatings: (a, d) pure FeCoNiCrMn coating, (b, e) Composite-1 coating, (c, f) Composite-2 coating.

sections. The wear tests were conducted by using a POD-2 pin-on-disc tribometer (CSEM Instruments, Switzerland) under a normal load of 5 N at room temperature. A WC-Co ball with a diameter of 5 mm was used as the counterpart material. The linear speed, rotation diameter and total sliding distance was set as 100 mm/s, 5 mm and 200 m, respectively. In addition, wear rate was calculated by the following equation [30]:

$$\frac{\omega = \pi \bullet D \bullet A}{F \bullet S}$$

where D is the diameter of the wear tracks (mm), F is the applied load (N) and S is the total sliding distance (m), A is the cross-sectional area of wear tracks (mm^2). In addition, a profilometer (Altisurf 500, Altimet, France) was used to measure the cross-sectional areas of the wear tracks.

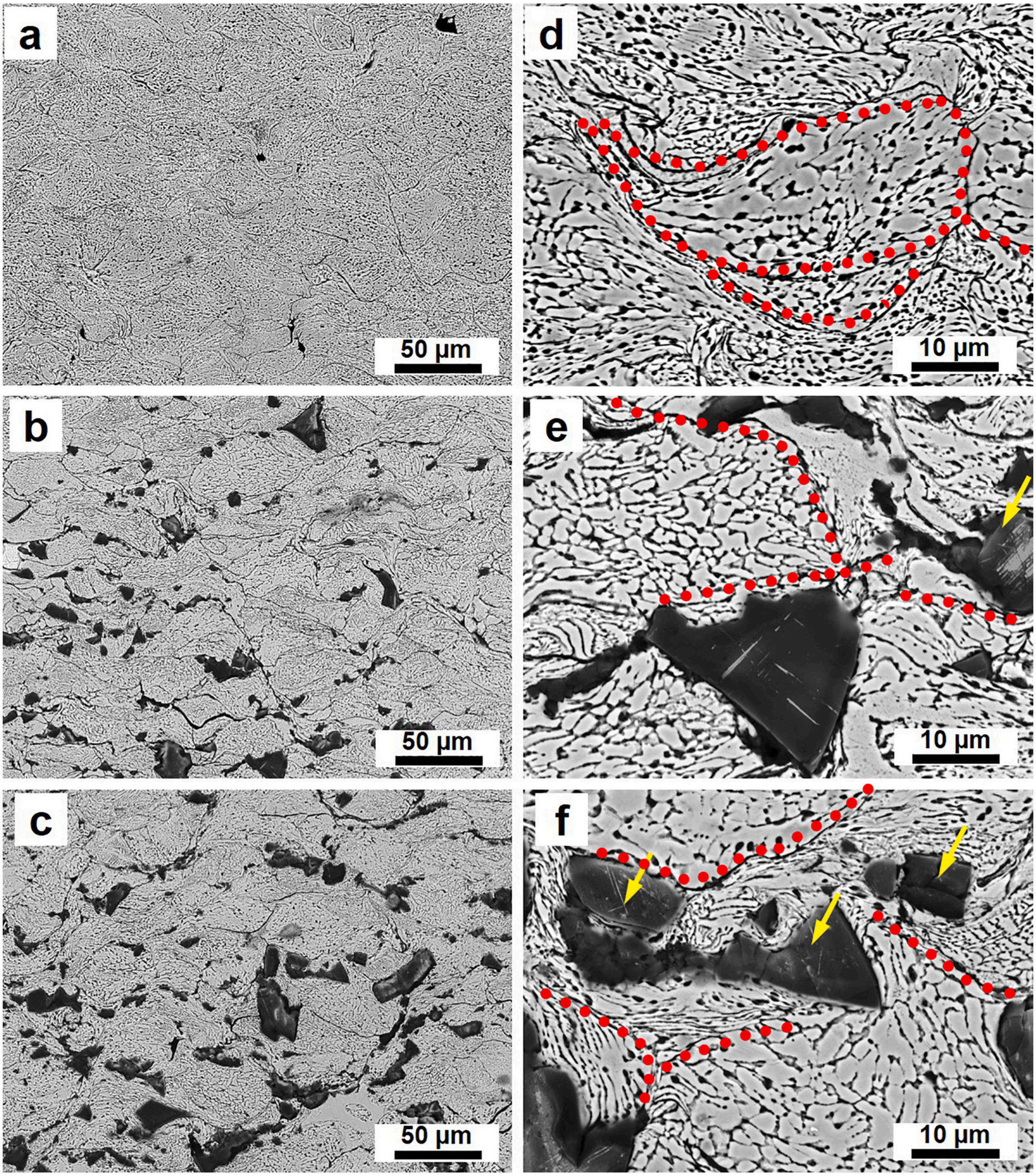

Fig. 4. Etched surface morphology showing the distribution of Al_2O_3 in FeCoNiCrMn composite coatings: (a, d) pure FeCoNiCrMn coating, (b, e) Composite-1 coating, (c, f) Composite-2 coating.

3. Results and discussion

3.1. Microstructure analysis

Fig. 3a–c show the SEM images (left column of Fig. 3) at the interface between the as-deposited coatings and the substrate. It can be observed that all the coatings showed well bonding with the Al alloy substrates as characterized by the clean interface that is free of gaps and cracks. Mechanical interlocking phenomenon could be observed along the interface between the coating and the substrate. Some particles penetrated the substrate and were tightly locked by the substrate material. The formation of mechanical interlocking is attributed to the severe plastic deformation of soft substrate material upon impact by hard FeCoNiCrMn particles. Mechanical interlocking is a typical characteristic of cold sprayed coatings, which can provide the coatings with high adhesion strength.

Fig. 3d–f show the cross-sectional SEM images (right column of Fig. 3) of the as-deposited coatings. It is clearly observed that the

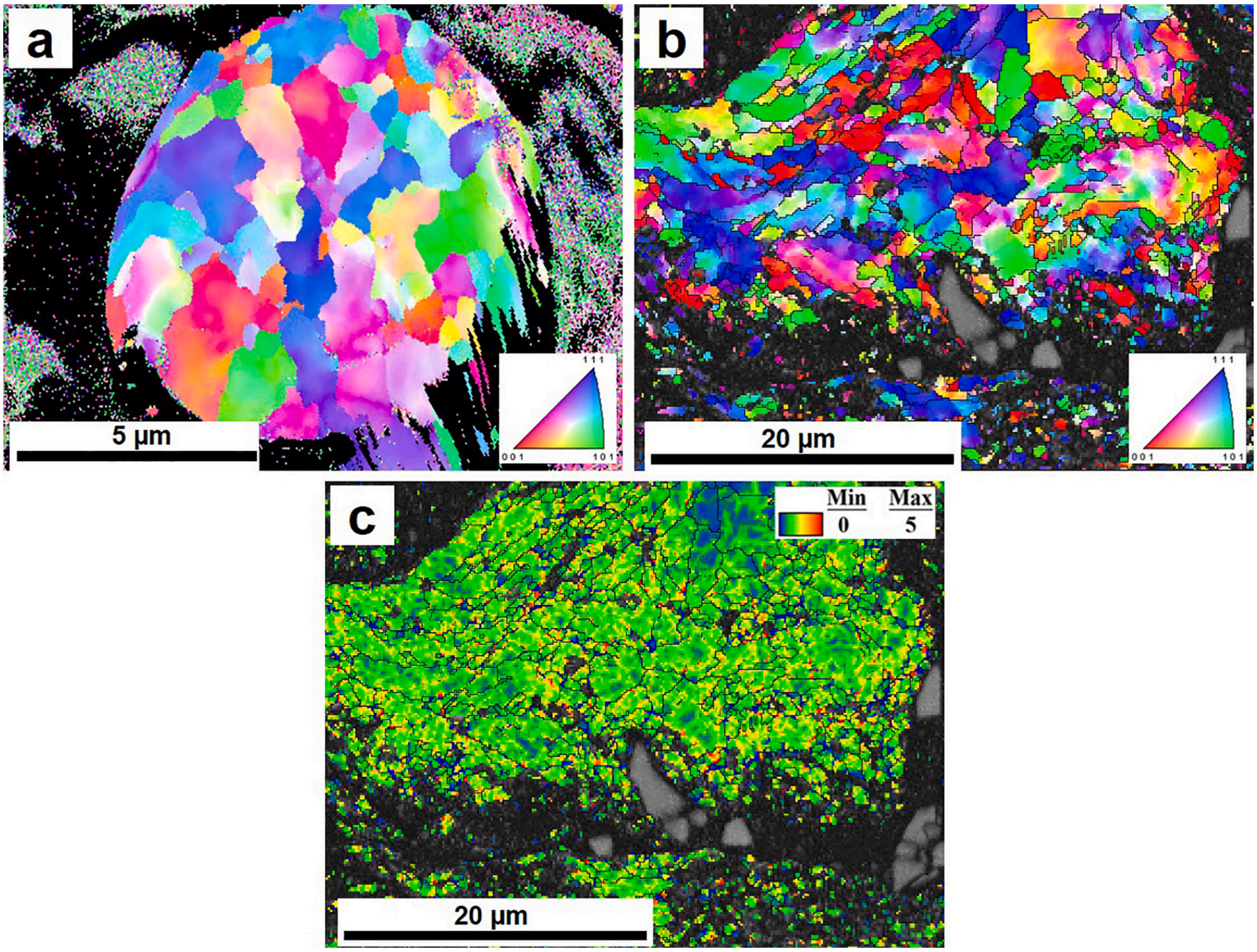

Fig. 5. EBSD IPF maps of (a) a single FeCoNiCrMn powder and (b) Composite-2 coating, and (c) KAM map of Composite-2 coating.

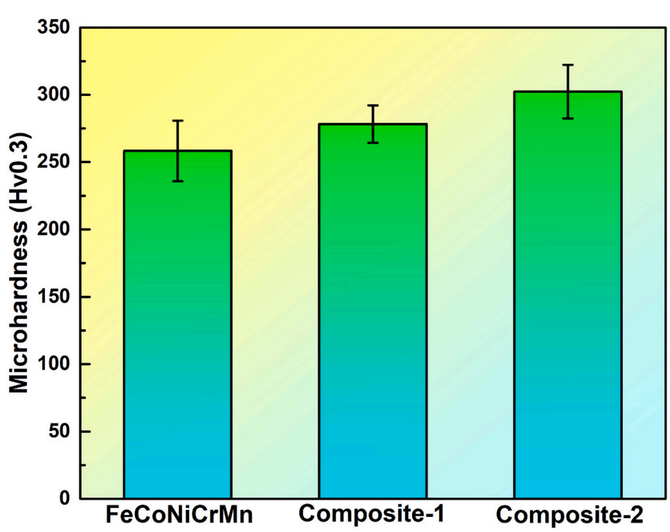

Fig. 6. Microhardness of the pure FeCoNiCrMn and composite coatings.

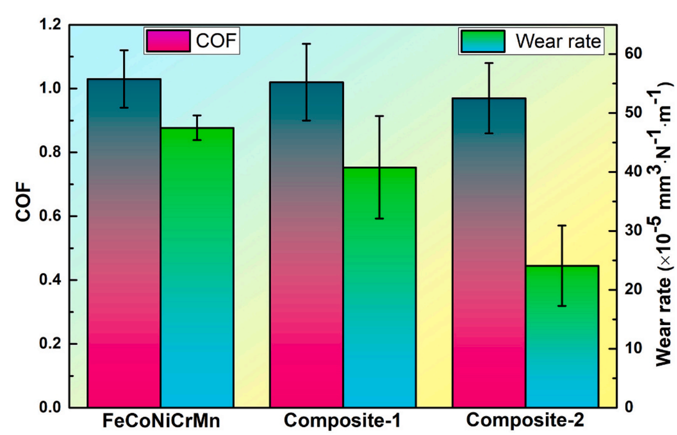

Fig. 7. COF and wear rate of the pure FeCoNiCrMn and composite coatings.

FeCoNiCrMn coatings presented a dense microstructure with only few pores as marked by yellow arrows and interparticle boundaries marked by red arrows. For the composite coatings, they also had dense microstructure as shown in Fig. 3e and f. Meanwhile, Al_2O_3 particles were well distributed in the FeCoNiCrMn matrix as marked by white arrows. However, interparticle gaps became more obvious in these composite coatings as marked by red arrows, especially in the Composite-2 coating which had higher content of Al_2O_3. Moreover, it is also found that the Al_2O_3 particles in the composite coatings were much smaller than in the feedstock due to occurrence of fragmentation of the Al_2O_3 particles during deposition process. In addition, the fraction of Al_2O_3 in the composite coatings significantly reduced by 63% for both the Composite-1 and the Composite-2 coatings due to the fragmentation and

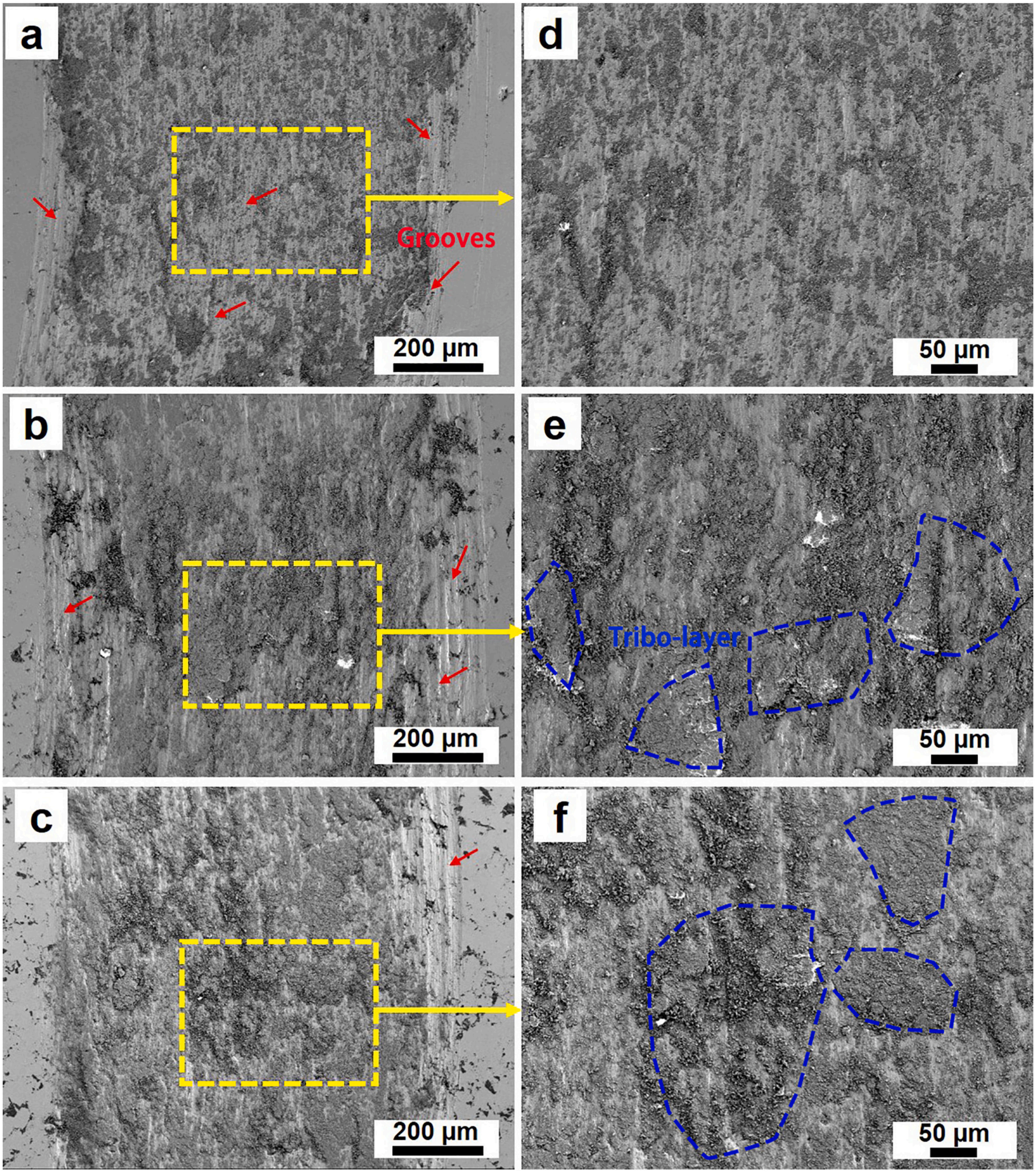

Fig. 8. Surface morphologies of the worn tracks: (a, d) Pure FeCoNiCrMn coating, (b, e) Composite-1 coating, (c, f) Composite-2 coating.

rebound of the Al_2O_3 particles, which is a common phenomenon for cold sprayed composite coatings.

The etched cross-sectional morphologies of the coatings are shown in Fig. 4, which could reveal the microstructure evolution during cold spray process. For all coatings, interparticle boundaries were revealed after etching as marked by red dotted line, which suggests that FeCoNiCrMn particles underwent severe plastic deformation after deposition. As for the composite coatings, all the Al_2O_3 particle were distributed along the inter-particle boundaries and cause secondary deformation of deposited FeCoNiCrMn particles. Moreover, cracks and tiny fragments could be found in some Al_2O_3 particles as marked by yellow arrows, which further confirms that Al_2O_3 particles underwent fragmentation during deposition due to high-velocity impact.

Fig. 5a and b show the inverse pole figure (IPF) map of a single FeCoNiCrMn powder and the Composite-2 coating at their cross-sections. Clearly, the grains close to the interparticle boundaries in the composite severely deformed and refined as compared to the grain in original powders, while the grains in the interior of the deformed particles were only elongated. This was attributed to the occurrence of dynamic recrystallization near the interparticle boundaries [28,31].

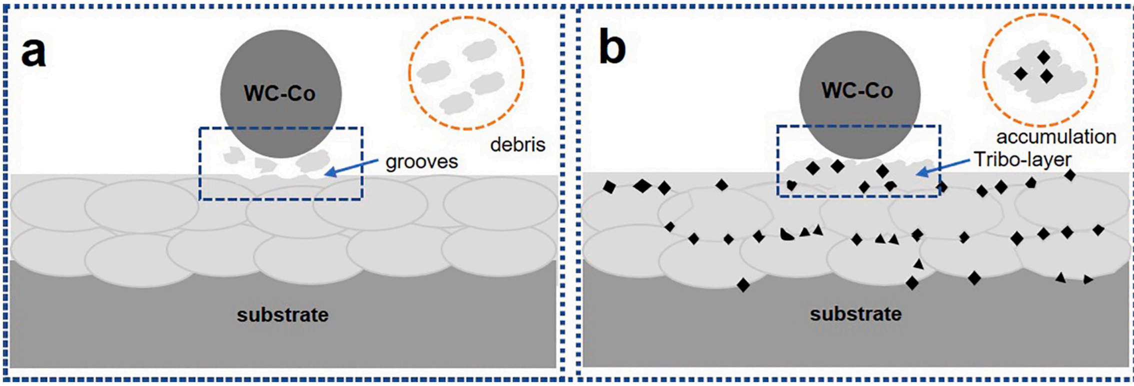

Fig. 9. Schematic diagram describing the wear mechanisms of (a) Pure FeCoNiCrMn and (b) composite coatings.

Fig. 5c shows the kernel average misorientation (KAM) maps of the Composite-2 coating. The KAM map was almost fully green, indicating that a dense network of dislocations/local strains was formed in the composite coating. This can be attributed to the heavily plastic deformation and work hardening effect during deposition process [32,33].

3.2. Microhardness and strengthening mechanism analysis

Fig. 6 presents the microhardness of the three coatings. It can be found that the microhardness of the coatings increased with increasing Al_2O_3 content, from 258.4 ± 22.6 $HV_{0.3}$ for the pure FeCoNiCrMn coating, to 278.3 ± 13.9 $HV_{0.3}$ for the Composite-1, and then to 302.4 ± 19.9 $HV_{0.3}$ for the Composite-2 coating. By comparing these values to the data reported in previous studies, the FeCoNiCrMn HEA coatings made in this work had higher hardness [34,35].

The enhanced microhardness can be attributed to the work hardening and grain refinement strengthening. Generally, higher particle impact velocity leads to denser coating with better mechanical properties due to the enhanced plastic deformation [25]. In this work, high-pressure He was used as propulsive gas to accelerate feedstock powders, which can result in a rather high particle impact velocity. In this case, particles could experience serve plastic deformation with localized regions undergoing ultra-high strain rate deformation. Therefore, the deposited particles had high dislocation density and microhardness. As for the composite coatings, the higher hardness can also be attributed to the dispersion strengthening effect of the well distributed Al_2O_3 particles which worked as hard skeleton to effectively protect the coating against external load.

3.3. Tribological properties and wear mechanism analysis

Fig. 7 shows the tribological properties including coefficient of friction (COF) and wear rate of the three coatings. It can be seen that the COF of the composite coatings did not show obvious variation as compared to the pure FeCoNiCrMn coating, but the wear rate greatly decreased with increasing the Al_2O_3 content. It is worth noting that the wear rate of the Composite-2 coating was nearly 50% lower than that of the pure FeCoNiCrMn coating. This result clearly illustrates the positive effect of Al_2O_3 particle on improving coating wear resistance. Moreover, all the HEA-based coatings had significant lower wear rates as compared to the substrate material 6082 Al alloy (12–22 × 10^{-3} $mm^3 \bullet N^{-1} \bullet m^{-1}$ as reported in Ref [36]), suggesting an excellent wear-resistance performance.

The surface morphologies of the worn tracks are presented in Fig. 8 to reveal the wear mechanism of the coatings. It can be seen that shallow plow grooves (marked by red arrows) parallel to the wear direction formed on the worn tracks of the pure FeCoNiCrMn coatings. Meanwhile, a number of tiny abrasive debris were also found on the worn surface (Fig. 8a and d). These features are typical characteristics of abrasive wear, which was normally caused by the micro-cutting from wear pairs and debris. As for the composite coatings, Al_2O_3 particles could be clearly seen outside the wear tracks. On the wear tracks, similar worn features to that for pure HEA coating could be observed, revealing that abrasive wear occurred during wear process. Moreover, more tiny debris were observed on the worn surfaces of the composite coatings (Fig. 8b and c). These debris went through accumulation and deformation, and then transformed into tribo-layer coated on the coating surface as shown in Fig. 8e and f. The tribo-layers were mechanical mixtures composed of HEA matrix debris and Al_2O_3 fragments or oxides as revealed in previous studies [18,30,37]. This phenomenon indicates that adhesive wear became the dominant wear mechanism for the composite coatings during the wear tests.

Fig. 9 shows the schematic diagram describing the wear process including the formation, accumulation and deformation of abrasive debris. As for the pure FeCoNiCrMn coatings, the WC-Co ball scratched the coating surface, and the coatings suffered abrasive wear damage to form debris due to their lower hardness than that of WC-Co ball (~1300 $HV_{0.3}$). Subsequently, the formed debris plough the coating surface and result in the formation of grooves as shown in Fig. 9a. As for the composite coatings, they had higher hardness than the pure FeCoNiCrMn coating. Thus, the composite coatings had higher capability to withstand abrasive wear damage at early wear stage. Even though, wear debris still formed and some Al_2O_3 fragments peeled off from the as-deposited composite coatings. And then the previously formed debris mechanically mixed with the Al_2O_3 fragments to form tribo-layer on the coating surface via smearing by WC-Co ball as shown in Fig. 9b. The tribo-layer coated on the worn surface is considered the main reason for the enhanced wear resistance of the composite coatings. In general, tribo-layers have higher hardness than matrix materials due to the formation of mechanical mixtures. According to the Archard's law, higher hardness results in better wear resistance due to the ploughing and micro-cutting effect of wear pairs [38]. Therefore, the tribo-layer coated on the coating surface can effectively prevent material loss from the cutting of wear pairs. Furthermore, the well distributed Al_2O_3 particles also help to prevent the loss of coating materials [39,40]. Thus, the composite coatings had better wear resistance as compared to the pure FeCoNiCrMn coating.

4. Conclusions

In this paper, cold spray was employed to deposit Al_2O_3 particles reinforced FeCoNiCrMn composite coatings. The effect of Al_2O_3 on the microstructure, hardness and tribological properties of the composite coatings was investigated. Based on the experimental results, it is found that cold spray is capable of fabricating HEA composite coatings with high density and well-distributed reinforcing particles. The composite coatings had higher hardness than the pure FeCoNiCrMn coating due to work hardening and grain size refinement and the well distributed Al_2O_3

particles in FeCoNiCrMn matrix. The composite coatings also demonstrated improved wear resistance as compared to the pure FeCoNiCrMn coating. The improved wear resistance can be attributed to the formation of tribo-layer which can effectively prevent material loss. And the main wear mechanism changed from abrasive wear for the pure FeCoNiCrMn coating to adhesive wear for the composite coatings.

CRediT authorship contribution statement

Yongming Zou: Writing – original draft, Investigation, Formal analysis. **Zhaoguo Qiu:** Resources, Writing – review & editing. **Chunjie Huang:** Resources, Investigation. **Dechang Zeng:** Supervision, Resources, Conceptualization. **Rocco Lupoi:** Resources. **Nannan Zhang:** Conceptualization, Writing – review & editing. **Shuo Yin:** Supervision, Conceptualization, Methodology, Formal analysis, Writing – review & editing.

Declaration of competing interest

The authors declare that they have no known competing financial interests or personal relationships that could have appeared to influence the work reported in this paper.

Acknowledgements

The authors would like to acknowledge the financial support from the China Scholarship Council (No. 202006150062) and International Cooperation Project of Guangdong Province (2021A0505030052).

References

[1] Y. Zhang, T.T. Zuo, Z. Tang, M.C. Gao, K.A. Dahmen, P.K. Liaw, Z.P. Lu, Microstructures and properties of high-entropy alloys, Prog. Mater. Sci. 61 (2014) 1–93.
[2] D.B. Miracle, O.N. Senkov, A critical review of high entropy alloys and related concepts, Acta Mater. 122 (2017) 448–511.
[3] M.-H. Tsai, J.-W. Yeh, High-entropy alloys: a critical review, Mater. Res. Lett. 2 (2014) 107–123.
[4] Y. Wu, F. Zhang, X. Yuan, H. Huang, X. Wen, Y. Wang, M. Zhang, H. Wu, X. Liu, H. Wang, S. Jiang, Z. Lu, Short-range ordering and its effects on mechanical properties of high-entropy alloys, J. Mater. Sci. Technol. 62 (2021) 214–220.
[5] J.M. Park, J. Choe, J.G. Kim, J.W. Bae, J. Moon, S. Yang, K.T. Kim, J.-H. Yu, H. S. Kim, Superior tensile properties of 1%C-CoCrFeMnNi high-entropy alloy additively manufactured by selective laser melting, Mater. Res. Lett. 8 (2020) 1–7.
[6] Z. Li, Interstitial equiatomic CoCrFeMnNi high-entropy alloys: carbon content, microstructure, and compositional homogeneity effects on deformation behavior, Acta Mater. 164 (2019) 400–412.
[7] H. Luo, Z. Li, A.M. Mingers, D. Raabe, Corrosion behavior of an equiatomic CoCrFeMnNi high-entropy alloy compared with 304 stainless steel in sulfuric acid solution, Corros. Sci. 134 (2018) 131–139.
[8] R. Li, P. Niu, T. Yuan, P. Cao, C. Chen, K. Zhou, Selective laser melting of an equiatomic CoCrFeMnNi high-entropy alloy: processability, non-equilibrium microstructure and mechanical property, J. Alloys Compd. 746 (2018) 125–134.
[9] Z. Cui, Z. Qin, P. Dong, Y. Mi, D. Gong, W. Li, Microstructure and corrosion properties of FeCoNiCrMn high entropy alloy coatings prepared by high speed laser cladding and ultrasonic surface mechanical rolling treatment, Mater. Lett. 259 (2020), 126769.
[10] M. Lobel, T. Lindner, T. Lampke, High-temperature wear behaviour of AlCoCrFeNiTi0.5 coatings produced by HVOF, Surf. Coat. Technol. 403 (2020), 126379.
[11] M. Lobel, T. Lindner, T. Lampke, High-temperature wear behaviour of AlCoCrFeNiTi0.5 coatings produced by HVOF, Surf. Coat. Technol. 403 (2020) 857–893.
[12] M. Löbel, T. Lindner, T. Mehner, L.-M. Rymer, S. Björklund, S. Joshi, T. Lampke, Microstructure and corrosion properties of AlCrFeCoNi high-entropy alloy coatings prepared by HVAF and HVOF, J. Therm. Spray Technol. 649 (2021) 1–9.
[13] L. Zendejas Medina, L. Riekehr, U. Jansson, Phase formation in magnetron sputtered CrMnFeCoNi high entropy alloy, Surf. Coat. Technol. 403 (2020), 126323.
[14] J.-K. Xiao, H. Tan, Y.-Q. Wu, J. Chen, C. Zhang, Microstructure and wear behavior of FeCoNiCrMn high entropy alloy coating deposited by plasma spraying, Surf. Coat. Technol. 385 (2020), 125430.
[15] J. Wang, B. Zhang, Y. Yu, Z. Zhang, S. Zhu, X. Lou, Z. Wang, Study of high temperature friction and wear performance of (CoCrFeMnNi)85Ti15 high-entropy alloy coating prepared by plasma cladding, Surf. Coat. Technol. 384 (2020), 125337.
[16] Q. Ye, K. Feng, Z. Li, F. Lu, R. Li, J. Huang, Y. Wu, Microstructure and corrosion properties of CrMnFeCoNi high entropy alloy coating, Appl. Surf. Sci. 396 (2017) 1420–1426.
[17] F. Ye, Z. Jiao, Y. Yuan, Precipitation behaviors and properties of micro-beam plasma arc cladded CoCrFeMnNi high-entropy alloy at elevated temperatures, Mater. Chem. Phys. 236 (2019), 121801.
[18] S. Zhu, Z. Zhang, B. Zhang, Y. Yu, Z. Wang, X. Zhang, B. Lu, Microstructure and properties of Al2O3-13wt.%TiO2-reinforced CoCrFeMnNi high-entropy alloy composite coatings prepared by plasma spraying, J. Therm. Spray Technol. 30 (2021) 772–786.
[19] Z. Zhang, B. Zhang, S. Zhu, Y. Yu, Z. Wang, X. Zhang, B. Lu, Microstructural characteristics and enhanced wear resistance of nanoscale Al2O3/13 wt%TiO2-reinforced CoCrFeMnNi high entropy coatings, Surf. Coat. Technol. 412 (2021), 127019.
[20] Y.B. Peng, W. Zhang, T.C. Li, M.Y. Zhang, L. Wang, Y. Song, S.H. Hu, Y. Hu, Microstructures and mechanical properties of FeCoCrNi high entropy alloy/WC reinforcing particles composite coatings prepared by laser cladding and plasma cladding, Int. J. Refract. Met. Hard Mater. 84 (2019), 105044.
[21] Y. Peng, W. Zhang, T. Li, M. Zhang, B. Liu, Y. Liu, L. Wang, S. Hu, Effect of WC content on microstructures and mechanical properties of FeCoCrNi high-entropy alloy/WC composite coatings by plasma cladding, Surf. Coat. Technol. 385 (2020), 125326.
[22] Z. Cai, X. Cui, G. Jin, Z. Liu, Y. Li, M. Dong, TEM observation on phase separation and interfaces of laser surface alloyed high-entropy alloy coating, Micron 103 (2017) 84–89.
[23] J.-E. Ahn, Y.-K. Kim, S.-H. Yoon, K.-A. Lee, Tuning the microstructure and mechanical properties of cold sprayed equiatomic CoCrFeMnNi high-entropy alloy coating layer, Met. Mater. Int. 27 (2020) 2406–2415.
[24] C. Chen, Y. Xie, L. Liu, R. Zhao, X. Jin, S. Li, R. Huang, J. Wang, H. Liao, Z. Ren, Cold spray additive manufacturing of invar 36 alloy: microstructure, thermal expansion and mechanical properties, J. Mater. Sci. Technol. 72 (2021) 39–51.
[25] N. Fan, J. Cizek, C. Huang, X. Xie, Z. Chlup, R. Jenkins, R. Lupoi, S. Yin, A new strategy for strengthening additively manufactured cold spray deposits through in-process densification, Addit. Manuf. 36 (2020), 101626.
[26] S. Yin, M. Hassani, Q. Xie, R. Lupoi, Unravelling the deposition mechanism of brittle particles in metal matrix composites fabricated via cold spray additive manufacturing, Scr. Mater. 194 (2021), 113614.
[27] Z. Zhang, D.H.L. Seng, M. Lin, S.L. Teo, T.L. Meng, C.J.J. Lee, Z.Q. Zhang, T. Ba, J. Y. Guo, K. Sundaravadivelu, P.K. Aw, J.S. Pan, Cold spray deposition of inconel 718 in comparison with atmospheric plasma spray deposition, Appl. Surf. Sci. 535 (2021), 147704.
[28] S. Yin, W. Li, B. Song, X. Yan, M. Kuang, Y. Xu, K. Wen, R. Lupoi, Deposition of FeCoNiCrMn high entropy alloy (HEA) coating via cold spraying, J. Mater. Sci. Technol. 35 (2019) 1003–1007.
[29] S. Yin, R. Jenkins, X. Yan, R. Lupoi, Microstructure and mechanical anisotropy of additively manufactured cold spray copper deposits, Mater. Sci. Eng. A 734 (2018) 67–76.
[30] Y. Zou, Z. Qiu, Z. Zheng, G. Wang, X. Yan, S. Yin, M. Liu, D. Zeng, Ex-situ additively manufactured FeCrMoCB/Cu bulk metallic glass composite with well wear resistance, Tribol. Int. 162 (2021), 107112.
[31] V. Luzin, K. Spencer, M.X. Zhang, Residual stress and thermo-mechanical properties of cold spray metal coatings, Acta Mater. 59 (2011) 1259–1270.
[32] N.H. Tariq, L. Gyansah, X. Qiu, H. Du, J.Q. Wang, B. Feng, D.S. Yan, T.Y. Xiong, Thermo-mechanical post-treatment: a strategic approach to improve microstructure and mechanical properties of cold spray additively manufactured composites, Mater. Des. 156 (2018) 287–299.
[33] A. Chaudhuri, Y. Raghupathy, D. Srinivasan, S. Suwas, C. Srivastava, Microstructural evolution of cold-sprayed inconel 625 superalloy coatings on low alloy steel substrate, Acta Mater. 129 (2017) 11–25.
[34] Z. Tong, H. Liu, J. Jiao, W. Zhou, Y. Yang, X. Ren, Laser additive manufacturing of CrMnFeCoNi high entropy alloy: microstructural evolution, high-temperature oxidation behavior and mechanism, Opt. Laser Technol. 130 (2020), 106326.
[35] B. Schuh, F. Mendez-Martin, B. Völker, E.P. George, H. Clemens, R. Pippan, A. Hohenwarter, Mechanical properties, microstructure and thermal stability of a nanocrystalline CoCrFeMnNi high-entropy alloy after severe plastic deformation, Acta Mater. 96 (2015) 258–268.
[36] H. Varol Özkavak, Ş. Şahin, M.F. Saraç, Z. Alkan, Comparison of wear properties of HVOF sprayed WC-co and WC-CoCr coatings on Al alloys, Mater. Res. Express 6 (2019), 096554.
[37] Y. Cui, J. Shen, S.M. Manladan, K. Geng, S. Hu, Wear resistance of FeCoCrNiMnAlx high-entropy alloy coatings at high temperature, Appl. Surf. Sci. 512 (2020), 145736.
[38] J.F. Archard, Contact and rubbing of flat surfaces, J. Appl. Phys. 24 (1953) 981–988.
[39] X. Jia, X. Ling, Influence of Al2O3 reinforcement on the abrasive wear characteristic of Al2O3/PA1010 composite coatings, Wear 258 (2005) 1342–1347.
[40] Z. Zhang, F. Liu, E.-H. Han, L. Xu, P.C. Uzoma, Effects of Al2O3 on the microstructures and corrosion behavior of low-pressure cold gas sprayed Al 2024-Al2O3 composite coatings on AA 2024-T3 substrate, Surf. Coat. Technol. 370 (2019) 53–68.